Communication

Dual-Polarized, High-Gain, and Low-Profile Magnetic Current Array Antenna

Yijing He, Yue Li, Wangyu Sun, and Zhijun Zhang

***Abstract*— In this communication, a dual-polarized 36-element (3 × 6 × 2) magnetic current array antenna is designed without using complex feeding network. Instead, a pair of differential feeds is adopted to excite the overall dual-polarized array within a low profile. Such a simple feeding strategy is achieved by using the TM_{90} mode of a microstrip antenna, which is loaded by 3 × 4 identical half-wavelength slots for each polarization. In this configuration, an in-phase 3 × 6 element single-polarized magnetic current array is achieved for high gain, but with narrow bandwidth due to the high-order mode. By trivially 90° rotating and combining, the proposed dual-polarized, high-gain, and low-profile magnetic current array is designed, constructed, and measured. Within a total size of $2.92\lambda_0 \times 2.92\lambda_0 \times 0.085\lambda_0$ (λ_0 is the free-space wavelength at the center frequency), the measured maximum gain is 15.5 dBi, also with the merits of low profile, low sidelobes, simple feeding, and high port isolation, exhibiting promising usage in MIMO and diversity applications.**

***Index Terms*— Differential feed, dual polarized antennas, magnetic current array, microstrip antennas, TM_{90} mode.**

I. Introduction

High-gain antenna has been widely desirable and applied in various modern wireless applications such as radar system, satellite communication, base station backhaul, and so on. To achieve high-gain antenna, many methods and techniques have been developed [1]–[24]. For example, an optical approach has been utilized to achieve various high-gain antennas such as reflector antenna (including reflected array) [1]–[4] and lens antenna (including transmitted array) [5]–[8]. These antennas usually require externally positioned feed source with a distance away from the radiating aperture. For designing a high-gain antenna in a volume-limited or planar integrated system, planar microstrip antenna array is often employed owing to its merits of low profile, easy integration, and low cost [9]. Microstrip antenna array usually needs complex feeding network to achieve excitations for all radiating elements, such as series feed or parallel feed. Series-fed network is suitable for the linear arranged microstrip antenna array [10]–[14]. For 2-D array configuration, parallel-fed network is often adopted [15]–[23], and the transmission losses must be considered when the array scale is large, thus limiting the gain improvement and decreasing the efficiency of the whole array.

Furthermore, dual-polarized property is usually required by high-gain antenna array owing to the merits of enhancing spectrum efficiency and increasing channel capacity [24]–[28]. The design complexity of the dual-polarized feeding networks is also greatly enhanced. The existing antenna array schemes achieving high gain and dual polarizations are usually equipped with complex feeding networks. It is a challenge to achieve high-gain and dual-polarized microstrip antenna array by using a simple feeding structure, which is the motivation of this communication.

Manuscript received September 5, 2018; revised October 29, 2018; accepted October 31, 2018. Date of publication November 27, 2018; date of current version February 5, 2019. This work was supported in part by the National Natural Science Foundation of China under Grant 61771280 and in part by the Natural Science Foundation of Beijing Manipulate under Contract 4182029. *(Corresponding author: Yue Li)*

The authors are with the Department of Electronic Engineering, Tsinghua University, Beijing 100084, China (e-mail: lyee@tsinghua.edu.cn).

Color versions of one or more of the figures in this communication are available online at http://ieeexplore.ieee.org.

Digital Object Identifier 10.1109/TAP.2018.2883609

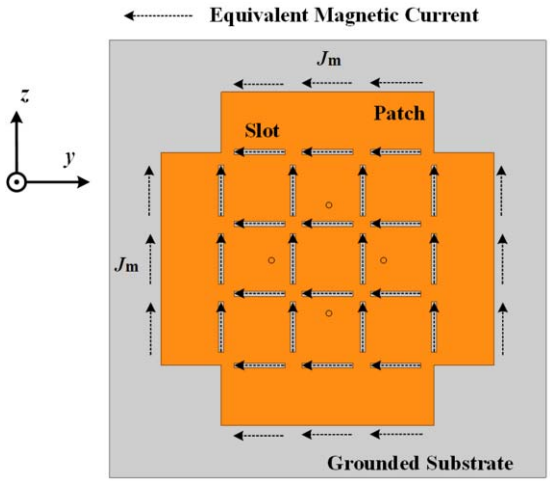

Fig. 1. General structure of the proposed dual-polarized magnetic current array.

Here, in this communication, we have proposed a high-gain, low-profile, and dual-polarized microstrip magnetic current array antenna with a pair of simple differential feeds. The simple feeding strategy is achieved by utilizing the TM_{90} mode of a microstrip antenna. Each polarization of the proposed antenna is loaded with 3 × 4 identical half-wavelength slots. By 90° rotation and combining, a dual-polarized magnetic current array antenna can be realized with the merits of high gain, low profile, simple feed, and high port isolation.

II. Antenna Design

A. Antenna Configuration and Evolution

Fig. 1 shows the general structure of the proposed dual-polarized magnetic current array antenna. Identical half-wavelength slots are loaded on the patch with nearly half-wavelength spacing between two adjacent elements. The proposed antenna is excited with a pair of differential feeds which utilize two Wilkinson 3 dB power dividers. The black arrows in Fig. 1 represent the $3 \times 6 \times 2$ element equivalent magnetic current array as the dual-polarized antenna. The proposed antenna is fabricated using the standard PCB process. Taconic TLX-8 dielectric substrate is used with a relative permittivity of 2.55, loss tangent of 0.002, and thickness of 1.524 mm. All the simulations of this communication were performed using the Ansoft high-frequency structure simulator.

The outstanding signature of the proposed antenna lies in that it achieves high gain using simple differential feeds instead of the complex and lossy feeding network in the conventional design. Fig. 2 illustrates the design evolution of the dual-polarized magnetic current array antenna, mainly containing three major steps. First, by etching four identical half-wavelength slots on a TM_{90}-mode

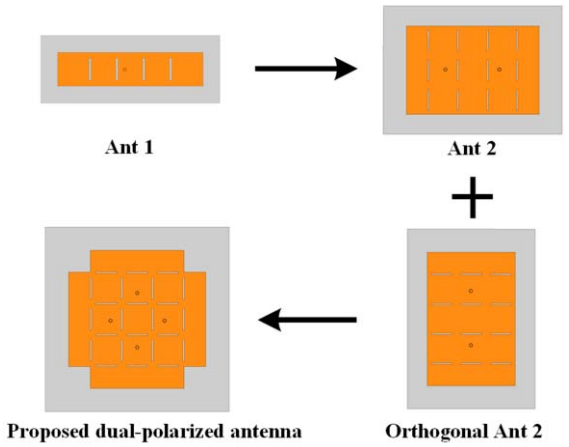

Fig. 2. Design evolution of the proposed magnetic current array antenna.

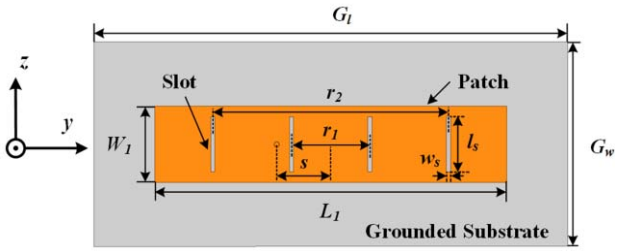

Fig. 3. Geometry of single-polarized subarray (Ant 1 shown in Fig. 2) operating at TM_{90} mode.

patch with nearly half-wavelength spacing, the electric fields on these slots and the two radiating apertures of the patch will oscillate in phase within a single resonant cavity. The four radiating slots and the two radiating apertures of the patch comprise a six-element microstrip magnetic current array antenna illustrated as Ant 1. Compared with conventional microstrip antenna operating at fundamental mode, Ant 1 can achieve a gain enhancement in broadside and simultaneously low sidelobes without using complex feeding network. Then, the second step is aimed to design a single-polarized antenna with further gain enhancement and simple feed based on Ant 1. Creatively, through arranging three subarrays as Ant 1 along the H-plane with spacing smaller than the width W_1 of Ant 1, they can be merged into one complete patch structure with single differential feed, as Ant 2. The final step achieves from the single-polarized case to the dual-polarized case. As shown in Fig. 2, by combining Ant 2 and its orthogonal one with a common center, a dual-polarized antenna containing 36 magnetic currents is constructed within a low profile.

B. Operating Principle

The operating principle and detailed geometry parameters of Ant 1, Ant 2, and the proposed dual-polarized antenna are discussed here. Fig. 3 presents the detailed structure of Ant 1, and Table I lists the geometry parameters of Ant 1. Ant 1 is based on a conventional microstrip antenna operating at TM_{90} mode. Fig. 4 shows the snapshot of the vector electric field distribution on the conventional microstrip antenna operating at TM_{90} mode. It can be observed that the electric field direction is alternating, and nine nulls exit along the y-direction of the patch. Then, four identical slots are etched on the positions of electric field nulls of the patch, whose locations are presented with four black circles. By these arrangements, strong radiating fields are generated in-phase with the two edges of the patch.

TABLE I
DIMENSIONS OF THE PROPOSED ANTENNA 1 (UNIT: MILLIMETERS)

L_1	W_1	r_1	r_2	s	l_s	W_s	G_l	G_w
54	11.2	12	34	9.1	8.1	0.6	70	30

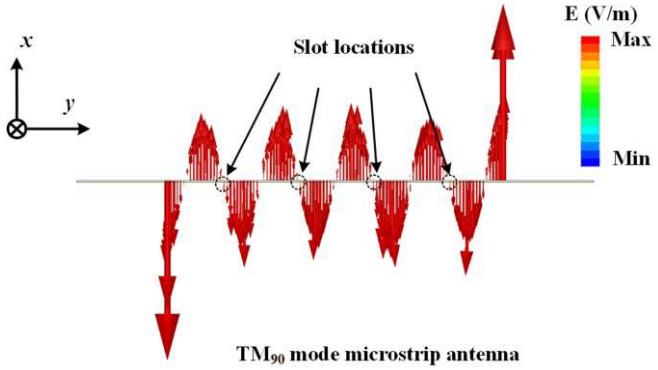

Fig. 4. Snapshot of electric vector field distribution on an ordinary microstrip antenna operating at TM_{90} mode (The black dotted circles mark the locations of the etched slots in Fig. 3).

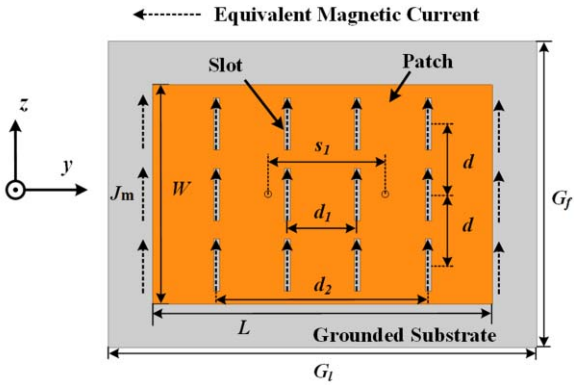

Fig. 5. Geometry of single-polarized array (Ant 2 shown in Fig. 2) made of three subarrays in Fig. 3 operating at TM_{90} mode.

Therefore, a six-element equivalent magnetic current array antenna as Ant 1 in Fig. 3 can be constructed within a single cavity using a single probe fed. The simple feeding structure benefits from the high-order mode of the microstrip antenna.

Then, by merging three subarrays as Ant 1 along the H-plane direction into one with identical array spacing d, Ant 2 in Fig. 5 can be constructed with differential feed. It should be noted that the subarray spacing d between the three subarrays is slightly smaller than the width W_1 of Ant 1. The detailed parameters of Ant 2 are presented in Table II. Although formed by three merged subarrays, here, Ant 2 is still operating at TM_{90} mode. In addition, due to the enlarged radiating aperture, the differential feeding technique must be employed to guarantee the whole antenna can be excited with near uniform-strength and in-phase property. Including the radiating edges on both ends of patch, a 3×6 element single-polarized magnetic current array antenna is formed with high gain and low sidelobes. The black arrows in Fig. 5 represent the equivalent 3×6 magnetic currents array. The simulated directivity of Ant 1 is shown in Fig. 6 with the red curve. The maximum directivity of Ant 1 reaches 12.5 dBi at 12.52 GHz. The black curve depicts the simulated directivity

TABLE II
DIMENSIONS OF THE PROPOSED ANTENNA 2 (UNIT: MILLIMETERS)

L	W	d	d_1	d_2	s_1	G_l	G_f
54	32.5	10.8	12	34	18.2	70	55

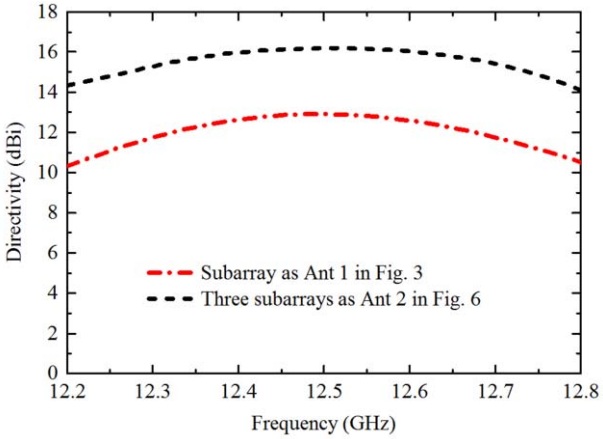

Fig. 6. Simulated directivity of the single-polarized microstrip antennas shown in Figs. 3 and 5, respectively.

TABLE III
DIMENSIONS OF THE PROPOSED DUAL-POLARIZED ANTENNA (UNIT: MILLIMETERS)

L_g	W_g	l	w	l_1	l_2	l_s	w_s	p	s_2
70	70	54	32.5	34.4	12.6	8.1	0.6	10.8	18.6

of Ant 2 with the ideal nondispersive differential excitation. The maximum value is 16.3 dBi at 12.52 GHz. Compared with Ant 1, 3.8 dB directivity enhancement is achieved for Ant 2.

Based on the proposed single-polarized magnetic current array as Ant 2, a dual-polarized antenna can be developed by combining Ant 2 with its orthogonal one. The structure feasibility of the dual-polarized antenna lies in that both the spacing between two neighboring slots along the E-plane and H-plane directions are almost half-wavelength.

Moreover, due to space orthogonality, the operating modes of the two polarizations of the antenna are almost independent with each other, ensuring the low cross-polarization property. The detailed structure and dimension of the proposed dual-polarized magnetic current array antenna are shown in Fig. 7, and the parameters listed in Table III. The complex current distribution in a whole period at 12.52 GHz is presented in Fig. 8, obtained when only the horizontal differential feeding port is fed. It can be observed that nine electric current maximums, i.e., nine electric field nulls exit along the horizontal direction, indicating the TM_{90} operating mode. Strong current distributions with half-wavelength mode can be clearly seen on all vertical slots. However, the horizontal slots are with very weak current distributions, implying the cross-polarization caused by these horizontal slots is small. This phenomenon explains why the operating modes of the two polarizations can keep almost independent though the two polarizations share the common structure. The orthogonality of the operating modes can lead to the high port isolation between the two polarizations.

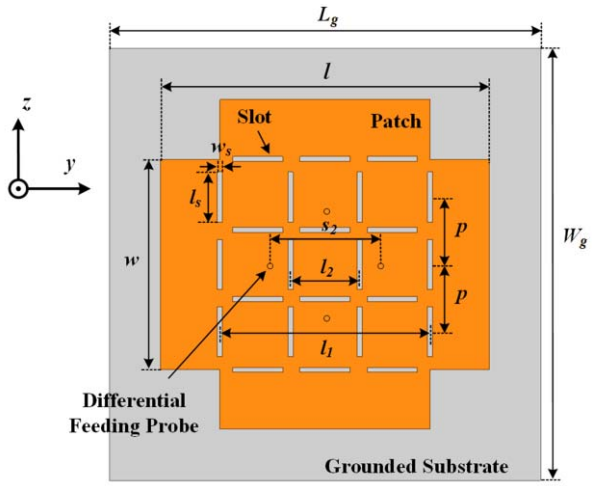

Fig. 7. Detailed geometry of the proposed dual-polarized magnetic current array antenna.

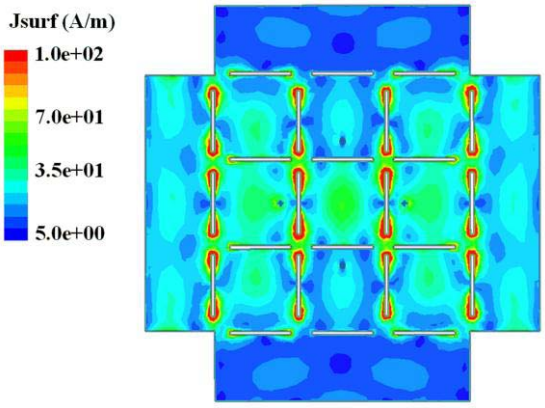

Fig. 8. Complex electric current distribution of the proposed array when only the horizontal differential ports are fed at 12.52 GHz.

Fig. 9 shows the perspective view of the final proposed dual-polarized magnetic current array antenna. The antenna contains two layers of dielectric substrate, with the upper layer supporting the radiating patch and the lower layer printed with two 3 dB Wilkinson differential feeds. Microstrip delay line is used to produce the antiphase excitation for each polarization. In addition, four metallic pins are used to achieve the transition from the microstrip line to the coaxial probe. The feeding positions of the four feeding probes are rotationally symmetric about the center of the antenna. Four circular clear holes with the diameter $Dr = 2.0$ mm are loaded on the middle metallic ground plane for the electrical connection of the four feeding pins from the lower feeding networks to the upper radiating patch. The diameter of these clear holes has been optimized to obtain good impedance matching. The lower substrate employs Taconic TLX-8 dielectric substrate with relative permittivity of 2.55, loss tangent of 0.002, and thickness of 0.508 mm. Fig. 10 presents the detailed structure of the two 3 dB Wilkinson differential feeding networks in the lower substrate. Here, two standard 100 Ω resistors are used to enhance the isolation between the differential feeding probes and absorb the reflected power. Moreover, the two differential feeding networks have identical quarter-wavelength impedance transformer structure. The 50 Ω microstrip feeding lines have a chamfered length of 1.3 mm, and the quarter-wavelength impedance transformers have a chamfered length of 0.4 mm. The detailed parameters of the two feeding networks are listed in Table IV.

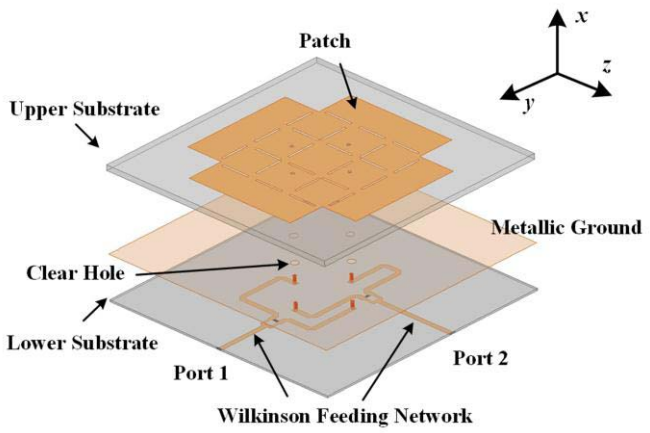

Fig. 9. Perspective view of the proposed dual-polarized magnetic current array antenna with the differential feeding network.

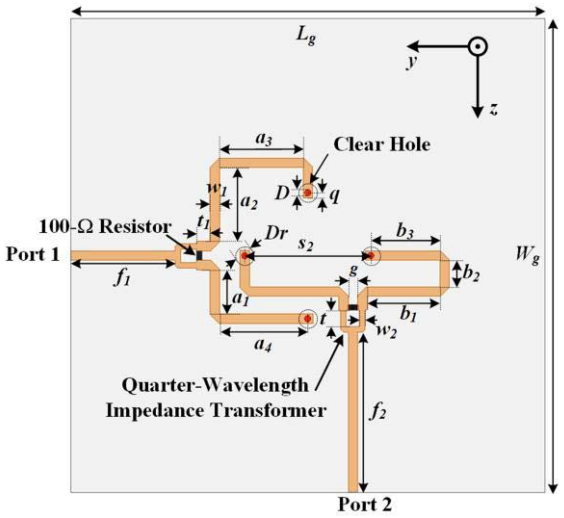

Fig. 10. Detailed parameters of the two 3 dB Wilkinson differential feeding networks.

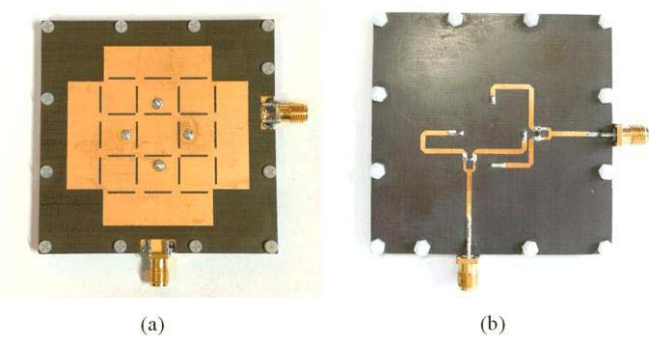

Fig. 11. (a) Top view and (b) bottom view of the fabricated prototype of the proposed dual-polarized magnetic current array antenna.

III. Experimental Results

To validate the high-gain signature of the proposed dual-polarized magnetic current array antenna, a prototype was fabricated and shown in Fig. 11. Fig. 11(a) and (b) shows the top and the bottom view of the fabricated prototype. Two 50 Ω coaxial SMA connectors were used to fed the two ports of the dual-polarized antenna. The S-parameters were measured with a vector network analyzer (Agilent E5071B),

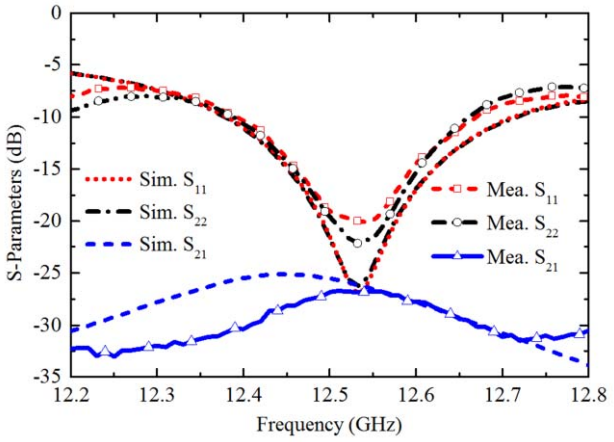

Fig. 12. Simulated and measured S-parameters of the prototype in Fig. 11.

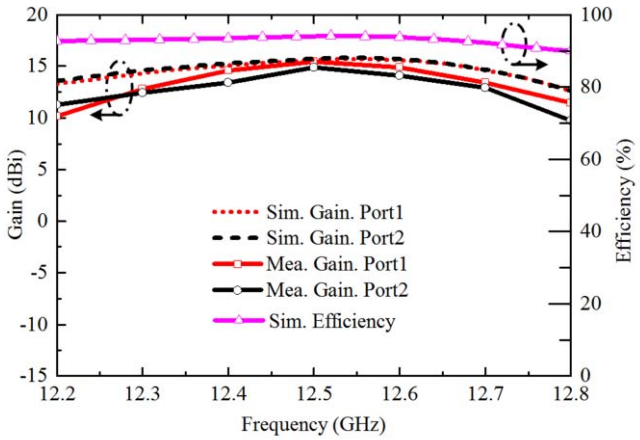

Fig. 13. Measured and simulated gain, and simulated radiation efficiency of the prototype in Fig. 11.

TABLE IV
DIMENSIONS OF THE DIFFERENTIAL FEEDING NETWORKS (UNIT: MILLIMETERS)

f_1	f_2	t	t_1	w_1	w_2	a_1	a_2	a_3
15.4	23.8	2.4	2.0	1.4	0.8	6.5	10.9	12.3
a_4	b_1	b_2	b_3	g	D	q	s_2	Dr
13.0	10.7	3.9	10.2	1.4	0.9	0.8	18.6	2.0

and the radiation patterns were measured in the far-field anechoic chamber.

The simulated and measured S-parameters of the proposed dual-polarized microstrip magnetic current array antenna are shown in Fig. 12. The simulated and measured results agree well with each other, and the measured reflection coefficients of the two ports are almost identical. The simulated −10 dB impedance bandwidth is from 12.38 to 12.72 GHz for both polarizations, and the measured one ranges from 12.39 to 12.68 GHz. The measured isolation between the two feeding ports almost keeps consistent with the simulated one, remaining lower than −27 dB. The high isolation between the two ports has verified the orthogonality of the two polarizations. The slight difference between the simulated and experimental results may

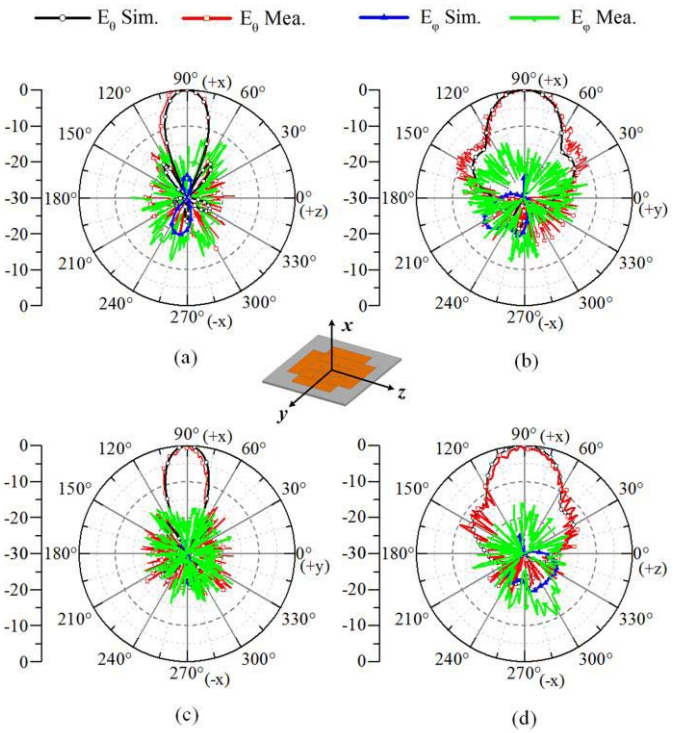

Fig. 14. Simulated and measured normalized radiation patterns of the proposed dual-polarized array fed through (a) Port 1 in *xoz* plane (b) Port 1 in *xoy* plane (c) Port 2 in *xoy* plane (d) Port 2 in *xoz* plane at 12.52 GHz.

TABLE V
COMPARISONS BETWEEN PROPOSED DESIGN AND REPORTED WORKS

Ref	Type	Feeding Design	Size (λ_0^3)	BW (%)	Max Gain (dBi)	Gain/Area ($1/\lambda_0^2$)
[20]	Single	Complex	20.2×20.2 × 0.08	6.4%	28.8	1.86
[21]	Single	Complex	3.57×3.57 ×0.08	25.5%	16.7	3.67
[22]	Single	Complex	47.2×47.2 ×0.22	24.8%	39.2	3.73
[23]	Single	Complex	4.0×2.8 ×0.04	21.2%	15.6	3.24
This work	**Dual**	**Simple**	**2.92×2.92 ×0.06**	**2.7%**	**15.5**	**4.16**

Single: single-polarized; Dual: dual-polarized

be resulted from the fabrication errors and fluctuations of dielectric constant.

The simulated and measured realized gains of the dual-polarized antenna are shown in Fig. 13 and agree quite well. The simulated and measured maximum realized gains of the proposed antenna with the feeding networks reach 15.9 and 15.5 dBi, respectively, at 12.52 GHz. The measured 3 dB gain bandwidth covers from 12.25 to 12.75 GHz for two polarizations. Due to the limitation of testing condition, only the simulated radiation efficiency of port 1 is given in Fig. 13. The radiation efficiency remains larger than 90% within the whole operating bandwidth with the maximum value of 94% at 12.52 GHz. The simulated and measured normalized radiation patterns at 12.52 GHz are shown in Fig. 14. Fig. 14(a) and (b) presents the E-plane and H-plane radiation patterns for z-polarization, and Fig. 14(c) and (d) is for y-polarization. The simulated and measured sidelobes are around −15 and −11 dB, respectively. The cross-polarization level is 20 dB lower than the copolarization level in the broadside. In addition, a size and performance comparison between the proposed antenna and other previously reported high-gain antennas using complex feeding networks is presented in Table V to highlight the merits of the proposed design. The comparison is performed in term of antenna structure, size, maximum gain, and the ratio of gain to area (which reflects the utilization ratio of the aperture). The effectiveness and scientificity of the gain to area have been well summarized in [29]. Moreover, the size here only includes the profile of antennas above the metallic reflector. It can be seen that though the proposed antenna is with relatively narrow bandwidth due to employing the higher order mode, it has the obvious higher ratio of gain to area compared with other designs using complex feeding networks. More importantly, the proposed antenna has the simple feeding network, which is less lossy and easy to design. The proposed method achieving high gain with simplified feeding network may be extended to a larger scale. In addition, the proposed design can be applied to dual-polarized operation with high isolation, which becomes even more difficult to realize for other high-gain antenna designs using complex feeding networks.

IV. CONCLUSION

This communication presents a high-gain, low-profile, and dual-polarized microstrip magnetic current array antenna. The main contribution of this communication is to achieve a high-gain (e.g., 15.5 dBi) magnetic current array antenna using simple differential feed. The novelty of such magnetic current array is using the slot-loaded TM_{90} mode of microstrip antenna and expanded into the dual-polarized configurations. By properly arranged the loaded slots, high ports isolation and low cross-polarization are achieved within a relatively low profile of 0.085 free-space wavelength at the center frequency, but with a narrow impedance bandwidth of 12.39 ∼ 12.68 GHz. The proposed dual-polarized antenna exhibits promising usage in MIMO and diversity systems.

REFERENCES

[1] M. Jiang, W. Hong, Y. Zhang, S. H. Yu, and H. Zhou, "A folded reflectarray antenna with a planar SIW slot array antenna as the primary source," *IEEE Trans. Antennas Propag.*, vol. 62, no. 7, pp. 3575–3583, Jul. 2014.
[2] R. Florencio, J. A. Encinar, R. R. Boix, V. Losada, and G. Toso, "Reflectarray Antennas for Dual Polarization and Broadband Telecom Satellite Applications," *IEEE Trans. Antennas Propag.*, vol. 63, no. 4, pp. 1234–1246, Apr. 2015.
[3] S. V. Hum and J. Perruisseau-Carrier, "Reconfigurable reflectarrays and array lenses for dynamic antenna beam control: A review," *IEEE Trans. Antennas Propag.*, vol. 62, no. 1, pp. 183–198, Jan. 2014.
[4] A. Yu, F. Yang, A. Z. Elsherbeni, J. Huang, and Y. Kim, "An offset-fed X-band reflectarray antenna using a modified element rotation technique," *IEEE Trans. Antennas Propag.*, vol. 60, no. 3, pp. 1619–1624, Mar. 2012.
[5] Q. Cheng, H. F. Ma, and T. J. Cui, "Broadband planar Luneburg lens based on complementary metamaterials," *Appl. Phys. Lett.*, vol. 95, no. 18, p. 181901, Nov. 2009.
[6] C. Pfeiffer and A. Grbic, "A printed, broadband luneburg lens antenna," *IEEE Trans. Antennas Propag.*, vol. 58, no. 9, pp. 3055–3059, Sep. 2010.
[7] C. Mateo-Segura, A. Dyke, H. Dyke, S. Haq, and Y. Hao, "Flat Luneburg lens via transformation optics for directive antenna applications," *IEEE Trans. Antennas Propag.*, vol. 62, no. 4, pp. 1945–1953, Apr. 2014.
[8] E. Erfani, M. Niroo-Jazi, and S. Tatu, "A high-gain broadband gradient refractive index metasurface lens antenna," *IEEE Trans. Antennas. Propag.*, vol. 64, no. 5, pp. 1968–1973, May 2016.
[9] A. G. Derneryd, "Microstrip array antenna," in *Proc. 6th Eur. Microw. Conf.*, Sep. 1976, pp. 339–343.
[10] A. Vallecchi and G. B. Gentili, "Design of dual-polarized series-fed microstrip arrays with low losses and high polarization purity," *IEEE Trans. Antennas Propag.*, vol. 53, no. 5, pp. 1791–1798, May 2005.

[11] K. Wincza and S. Gruszczynski, "Microstrip antenna arrays fed by a series-parallel slot-coupled feeding network," *IEEE Antennas Wireless Propag. Lett.*, vol. 10, pp. 991–994, 2011.
[12] T. Yuan, N. Yuan, and L. W. Li, "A novel series-fed taper antenna array design," *IEEE Antennas Wireless Propag. Lett.*, vol. 7, no. , pp. 362–365, 2008.
[13] K. Wincza, S. Gruszczynski, and J. Borgosz, "Microstrip antenna array with series-fed 'through-element' coupled patches," *Electron. Lett.*, vol. 43, no. 9, pp. 487–489, Apr. 2007.
[14] I. Slomian, K. Wincza, and S. Gruszczynski, "Series-fed microstrip antenna array with inclined-slot couplers as three-way power dividers," *IEEE Antennas Wireless Propag. Lett.*, vol. 12, pp. 62–64, 2013.
[15] P. S. Hall and C. M. Hall, "Coplanar corporate feed effects in microstrip patch array design," *IEE Proc. H-Microw., Antennas Propag.*, vol. 135, no. 3, pp. 180–186, Jun. 1988.
[16] H. D. Chen, C. Y. D. Sim, J. Y. Wu, and T. W. Chiu, "Broadband high-gain microstrip array antennas for WiMAX base station," *IEEE Trans. Antennas Propag.*, vol. 60, no. 8, pp. 3977–3980, Aug. 2012.
[17] J. Huang, "A Ka-band circularly polarized high-gain microstrip array antenna," *IEEE Trans. Antennas Propag.*, vol. 43, no. 1, pp. 113–116, Jan. 1995.
[18] R. Lian, Z. Wang, Y. Yin, J. Wu, and X. Song, "Design of a low-profile dual-polarized stepped slot antenna array for base station," *IEEE Antennas Wireless Propag. Lett.*, vol. 15, pp. 362–365, 2016.
[19] Y. Wang and Z. Du, "Dual-polarized slot-coupled microstrip antenna array with stable active element pattern," *IEEE Trans. Antennas Propag.*, vol. 63, no. 9, pp. 4239–4244, Sep. 2015.
[20] Y. J. Cheng, Y. X. Guo, and Z. G. Lin, "W-band large-scale high-gain planar integrated antenna array," *IEEE Trans. Antennas Propag.*, vol. 62, no. 6, pp. 3370–3373, Jun. 2014.
[21] M. J. Li and K. M. Luk, "Low-cost wideband microstrip antenna array for 60-GHz applications," *IEEE Trans. Antennas Propag.*, vol. 62, no. 6, pp. 3012–3018, Jun. 2014.
[22] J. Wu, Y. J. Cheng, and Y. Fan, "A wideband high-gain high-efficiency hybrid integrated plate array antenna for V-band inter-satellite links," *IEEE Trans. Antennas Propag.*, vol. 63, no. 4, pp. 1225–1233, Apr. 2015.
[23] W. Yang, K. Ma, K. S. Yeo, and W. M. Lim, "A compact high-performance patch antenna array for 60-GHz applications," *IEEE Antennas Wireless Propag. Lett.*, vol. 15, pp. 313–316, Feb. 2016.
[24] Y. Li, Z. J. Zhang, J. F. Zheng, and Z. H. Feng, "Compact azimuthal omnidirectional dual-polarized antenna using highly isolated colocated slots," *IEEE Trans. Antennas Propag.*, vol. 60, no. 9, pp. 4037–4045, Sep. 2012.
[25] H. Zhai, Y. Zang, and L. Li, "A low-profile dual-polarized high-isolation MIMO antenna arrays for wideband base-station applications," *IEEE Trans. Antennas Propag.*, vol. 66, no. 1, pp. 191–202, Jan. 2018.
[26] H. Wong, K.-L. Lau, and K.-M. Luk, "Design of dual-polarized L-probe patch antenna arrays with high isolation," *IEEE Trans. Antennas Propag.*, vol. 52, no. 1, pp. 45–52, Jan. 2004.
[27] M. A. Jensen and J. W. Wallace, "A review of antennas and propagation for MIMO wireless communications," *IEEE Trans. Antennas Propag.*, vol. 52, no. 11, pp. 2810–2824, Nov. 2004.
[28] P.-S. Kildal and K. Rosengren, "Correlation and capacity of MIMO systems and mutual coupling, radiation efficiency, and diversity gain of their antennas: Simulations and measurements in a reverberation chamber," *IEEE Commun. Mag.*, vol. 42, no. 12, pp. 104–112, Dec. 2004.
[29] D. F. Sievenpiper *et al.*, "Experimental validation of performance limits and design guidelines for small antennas," *IEEE Trans. Antennas Propag.*, vol. 60, no. 1, pp. 8–19, Jan. 2012.